

Graphical Models for Discrete and Continuous Data

Rui Zhuang

Department of Biostatistics, University of Washington
and

Noah Simon

Department of Biostatistics, University of Washington
and

Johannes Lederer

Department of Mathematics, Ruhr-University Bochum

June 18, 2019

Abstract

We introduce a general framework for undirected graphical models. It generalizes Gaussian graphical models to a wide range of continuous, discrete, and combinations of different types of data. The models in the framework, called exponential trace models, are amenable to estimation based on maximum likelihood. We introduce a sampling-based approximation algorithm for computing the maximum likelihood estimator, and we apply this pipeline to learn simultaneous neural activities from spike data.

Keywords: Non-Gaussian Data, Graphical Models, Maximum Likelihood Estimation

1 Introduction

Gaussian graphical models (Drton & Maathuis 2016, Lauritzen 1996, Wainwright & Jordan 2008) describe the dependence structures in normally distributed random vectors. These models have become increasingly popular in the sciences, because their representation of the dependencies is lucid and can be readily estimated. For a brief overview, consider a

random vector $X \in \mathbb{R}^p$ that follows a centered normal distribution with density

$$f_{\Sigma}(\mathbf{x}) = \frac{1}{(2\pi)^{p/2} \sqrt{|\Sigma|}} e^{-\mathbf{x}^T \Sigma^{-1} \mathbf{x} / 2} \quad (1)$$

with respect to Lebesgue measure, where the population covariance $\Sigma \in \mathbb{R}^{p \times p}$ is a symmetric and positive definite matrix. Gaussian graphical models associate these densities with a graph (V, E) that has vertex set $V := \{1, \dots, p\}$ and edge set $E := \{(i, j) : i, j \in \{1, \dots, p\}, i \neq j, \Sigma_{ij}^{-1} \neq 0\}$. The graph encodes the dependence structure of X in the sense that any two entries $X_i, X_j, i \neq j$, are conditionally independent given all other entries if and only if $(i, j) \notin E$. A natural and straightforward estimator of Σ^{-1} , and thus of E , is the inverse of the empirical covariance, which is also the maximum likelihood estimator. Inference can then be approached via the quantiles of the normal distribution.

The problem with Gaussian graphical models is that in practice, data often violate the normality assumption. Data can be discrete, heavy-tailed, restricted to positive values, or deviate from normality in other ways. Graphical models for some types of non-Gaussian data have been developed, including copula-based models (Gu et al. 2015, Liu et al. 2012, 2009, Xue & Zou 2012), score matching approach (Lin et al. 2016, Yu et al. 2019), Ising models (Brush 1967, Lenz 1920), and multinomial extensions of the Ising models (Loh & Wainwright 2013). However, there is no general framework that comprises different data types including finite and infinite count data, potentially heavy-tailed continuous data, and combinations of discrete and continuous data and at the same time, ensures a rigid theoretical structure.

We make three main contributions in this paper:

- We formulate a general framework for undirected graphical models that both encompasses previously studied and new models for continuous, discrete, and combined data types.
- We show that maximum likelihood is based on a convex and smooth optimization function and provides consistent estimation and inference for the model parameters in the framework.
- We establish a sampling-based approximation algorithm for computing the maximum likelihood estimator.

Let us have a glance at the framework. For this, we start with the Gaussian densities (1). Our first observation is that $-\mathbf{x}^\top \Sigma^{-1} \mathbf{x} / 2 = -\langle \Sigma^{-1}, \mathbf{x} \mathbf{x}^\top / 2 \rangle_{\text{tr}}$, where $\langle \cdot, \cdot \rangle_{\text{tr}}$ is the trace inner product. This formulation looks “somewhat less revealing” (Eaton 2007, Page 125) on first sight, but it has two conceptual advantages. First, we argue that writing the parameters and the data as algebraic duals of each other makes their relationship more symmetric. Second, we argue that it is a good starting point for generalizations. For this, we take the viewpoint that the exponents in the densities are linear functions of the matrix $\mathbf{x} \mathbf{x}^\top / 2$, and then replace this matrix by a general matrix-valued function T of \mathbf{x} . Our second observation is that the fundamental quantity in the family of Gaussian graphical models is the inverse covariance matrix Σ^{-1} rather than the covariance matrix Σ itself. This suggests a reparametrization of the model using the matrix Σ^{-1} , which is then replaced by a general matrix M . This subtlety is important: as we will see later, the matrix M contains all information about the dependence structure of X , while the equality of M^{-1} and the covariance matrix is a mere coincidence in the Gaussian case. With these two observations in mind, and denoting the log-normalization by $\gamma(M)$, with $\gamma(M) = \log((2\pi)^p |M^{-1}|) / 2$ in the Gaussian case, we can then generalize the densities (1) to

$$f_M(\mathbf{x}) = e^{-\langle M, T(\mathbf{x}) \rangle_{\text{tr}} - \gamma(M)}$$

with respect to an arbitrary σ -finite measure ν , and with $M, T \in \mathbb{R}^{q \times q}$ a matrix-valued parameter and data function, respectively. While additional data terms can be absorbed in the measure ν , it is sometimes illustrative to write them explicitly. We thus consider distributions with densities of the form

$$f_M(\mathbf{x}) = e^{-\langle M, T(\mathbf{x}) \rangle_{\text{tr}} + \xi(\mathbf{x}) - \gamma(M)},$$

where $\xi(\mathbf{x})$ depends on \mathbf{x} only. These densities form an exponential family indexed by M and are called exponential trace models in the following for convenience.

We recall that the well-known pairwise interaction models can also be written in exponential form, but there are important differences to the above formulation. First, pairwise interaction models and exponential trace models are not sub-classes of one another: exponential trace models are not limited to pairwise interactions, while pairwise interaction models are not limited to canonical parameterizations. Yet, importantly, exponential trace

models generalize pairwise interaction models in the sense that all generic examples of pairwise interaction models are encompassed. We also highlight that in contrast to pairwise interaction models, we allow for $q \neq p$, which helps for concise formulations of mixed graphical models, for example. In general, we argue that the exponential trace framework is a practical starting point for general studies of graphical models, because it comprises a very large variety of examples and still ensures a firm theoretical structure.

We carefully specify and study the described distributions in the following sections. Section 2 contains the proposed framework: we define the densities in Section 2.1, and we discuss a variety of examples in Sections 2.2 and 2.3. Section 3 is focused on estimation: we discuss the maximum likelihood estimator for the model parameters in Section 3.1, and we introduce a numerical algorithm in Sections 3.2. Section 4 shows simulation results for different types of data. Section 5 applies the method to neural spike data. We conclude the paper with a discussion in Section 6. The proofs are deferred to the Appendix.

Notation

For matrices $A, B \in \mathbb{R}^{s \times t}$, $s, t \in \{1, 2, \dots\}$, we denote the trace inner product (or Frobenius inner product) by

$$\langle A, B \rangle_{\text{tr}} := \text{tr}(A^\top B) = \sum_{i=1}^s \sum_{j=1}^t A_{ij} B_{ij}$$

and the corresponding norm by

$$\|A\|_{\text{tr}} := \sqrt{\langle A, A \rangle_{\text{tr}}} = \sqrt{\sum_{i=1}^s \sum_{j=1}^t A_{ij}^2}.$$

We consider random vectors $X = (X_1, \dots, X_p)^\top \in \mathbb{R}^p$. We denote random vectors and their realizations by upper case letters such as X and arguments of functions by lower case, boldface letters such as \mathbf{x} . Given a set $S \subset \{1, \dots, p\}$, we denote by $X_S \in \mathbb{R}^{|S|}$ the vector that consists of the coordinates of X with indices in S , and we set $X_{-S} := X_{S^c} \in \mathbb{R}^{p-|S|}$. Independence of two elements X_i and X_j , $i \neq j$, is denoted by $X_i \perp X_j$; conditional independence of X_i and X_j given all other elements is denoted by $X_i \perp\!\!\!\perp X_j | X_{-\{i,j\}}$.

2 Framework

We first discuss our framework. In Section 2.1, we formulate the densities. In Section 2.2, we show that these densities apply to standard examples of graphical models. In Section 2.3, we study additional examples.

2.1 Exponential Trace Models

In this section, we formulate probabilistic models for vector-valued observations that have dependent coordinates. Specifically, we consider arbitrary (non-empty) finite or continuous domains $\mathcal{D} \subset \mathbb{R}^p$ and random vectors $X \in \mathcal{D}$ that have densities of the form

$$f_M(\mathbf{x}) := e^{-\langle M, T(\mathbf{x}) \rangle_{\text{tr}} + \xi(\mathbf{x}) - \gamma(M)} \quad (2)$$

with respect to some σ -finite measure ν on \mathcal{D} . For reference, we call these models exponential trace models.

We begin by specifying the different components of our model. The densities are indexed by $M \in \mathfrak{M}$, where \mathfrak{M} is a subset of

$$\mathfrak{M}^* := \text{interior}\{M \in \mathbb{R}^{q \times q} : \gamma(M) < \infty\}.$$

Unlike conventional frameworks, we do not require $q = p$, with the advantage of concise formulations of mixture models, for example. In generic applications, M comprises the dependence structure of X and determines if two coordinates X_i and X_j are positively or negatively correlated. We will discuss these aspects in the next sections. The arguably most important note here is that the integrability condition $\gamma(M) < \infty$ is feasible. In particular, our framework provides natural formulations of models that avoid unreasonable restrictions on the parameter space. It is best to see this in specific examples, so that we defer to later.

Next, the data enters the model via a matrix-valued function

$$\begin{aligned} T : \mathcal{D} &\rightarrow \mathbb{R}^{q \times q} \\ \mathbf{x} &\mapsto T(\mathbf{x}) \end{aligned}$$

and a real-valued function

$$\begin{aligned}\xi &: \mathcal{D} \rightarrow \mathbb{R} \\ \mathbf{x} &\mapsto \xi(\mathbf{x}),\end{aligned}$$

and $\gamma(M)$ is the normalization defined as

$$\gamma(M) := \log \int_{\mathcal{D}} e^{-\langle M, T(\mathbf{x}) \rangle_{\text{tr}} + \xi(\mathbf{x})} d\nu.$$

We finally have to impose two technical assumptions on the parameter space. Our first assumption is that the function $M \mapsto f_M$ of \mathfrak{M} to the densities with respect to the measure ν is bijective. Sufficient conditions for this are provided in (Berk 1972, Page 199) and (Johansen 1979, Definition 1.3); we stress, however, that the bijection is required here only on \mathfrak{M} rather than on the full set \mathfrak{M}^* . Our second assumption is that \mathfrak{M} is convex and that \mathfrak{M} is open with respect to an affine subspace of $\mathbb{R}^{q \times q}$. The two assumptions ensure, in particular, that the parameter M is identifiable and has a compact and “full-dimensional” neighborhood in an affine subspace of $\mathbb{R}^{q \times q}$. Importantly, however, the assumptions are mild enough to allow for overparametrizations in the sense that \mathfrak{M} does not have to be open in $\mathbb{R}^{q \times q}$; a typical example is \mathfrak{M} equal to the set of symmetric matrices, seen in Sections 2.2 and 2.3.

The exponential family formulation equips the framework with desirable structure. In particular, we can derive the following.

Lemma 2.1. *The following two properties are satisfied.*

1. *The set \mathfrak{M}^* is convex;*
2. *for any $M \in \mathfrak{M}^*$, the coordinates of $T(X)$ have moments of all orders with respect to f_M .*

Property 1 ensures that $\mathfrak{M} = \mathfrak{M}^*$ satisfies the above assumption about \mathfrak{M} and Property 2 ensures concentration of the maximum likelihood estimator discussed later.

2.2 Standard Graphical Models

The goal of this section is to demonstrate that standard graphical models, such as Ising models with binary and m -ary responses and Gaussian and non-paranormal graphical mod-

els, fit the exponential trace framework. In combination with the results in Section 3, this shows in particular that standard graphical models are automatically equipped with more structure than suggested by common pairwise interaction formulations.

For the standard models, it is sufficient to consider $q = p$, $T_{ij}(\mathbf{x}) \equiv T_{ij}(x_i, x_j)$, and $\xi(\mathbf{x}) = \sum_{j=1}^p \xi_j(x_j)$. Given M , we then define a graph $G := (V, E)$, where $V := \{1, \dots, p\}$ is the vertex (or node) set and $E := \{(i, j) : i, j \in V, i \neq j, M_{ij} \neq 0\}$ the edge set. Two matrices $M, M' \in \mathfrak{M} \subset \mathbb{R}^{p \times p}$ correspond to the same graph if and only if their non-zero patterns are the same. In view of the examples below, we are particularly interested in symmetric dependence structures, that is, we consider symmetric matrices M in what follows. Then, also the edge set E is symmetric, that is, $(i, j) \in E$ if and only if $(j, i) \in E$, and the graph G is called undirected.

The corresponding models f_M are a special case of pairwise interaction models (pairwise Markov networks). Assuming that ν is a product measure, a density h with respect to ν is a pairwise interaction model if it can be written in the form

$$h(\mathbf{x}) = \prod_{i,j=1}^p h_{ij}(x_i, x_j)$$

with positive functions h_{ij} . This means that the densities of pairwise interaction models can be written as products of terms that depend on at most two coordinates.

The graph G now encodes the conditional dependence structure, as one can show by applying the Hammersley-Clifford theorem (Besag 1974, Grimmett 1973). The theorem implies that for a strictly positive density $h(\mathbf{x})$ with respect to a product measure, two elements X_i, X_j are conditionally independent given all other coordinates if and only if we can write $h(\mathbf{x}) = h^1(\mathbf{x}_{-i})h^2(\mathbf{x}_{-j})$, where h^1, h^2 are positive functions. For the described densities in our framework, we can write $f_M(\mathbf{x}) = f_M^1(\mathbf{x}_{-i})f_M^2(\mathbf{x}_{-j})$ with positive functions f_M^1, f_M^2 if and only if $M_{ij} = 0$. By the above definition of the graph associated with M , the latter is equivalent to $(i, j) \notin E$. We thus find

$$X_i \perp\!\!\!\perp X_j | X_{-\{i,j\}} \quad \text{if and only if} \quad (i, j) \notin E,$$

meaning that the conditional dependence structure of X is represented by the edge set E .

The graph G also determines the unconditional dependence structure. To illustrate this, we define \overline{E} as the set of all connected components in M , that is, $(i, j) \in \overline{E}$ if and only

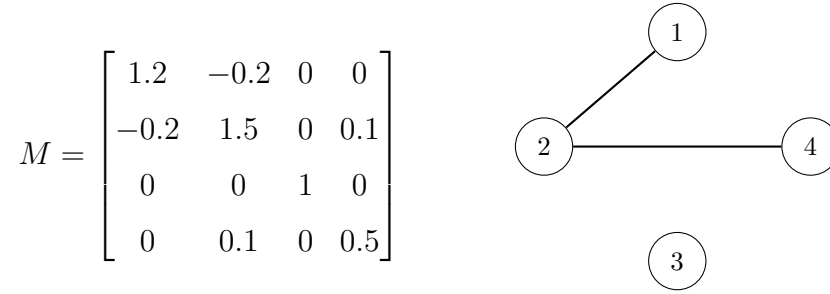


Figure 1: Example of a matrix M (left) and the corresponding graph G (right). The vertex set of the graph is $V = \{1, 2, 3, 4\}$, the edge set of the graph is $E = \{(1, 2), (2, 1), (2, 4), (4, 2)\}$. The enlarged edge set is $\bar{E} = E \cup \{(1, 4), (4, 1)\}$. For example, X_1 and X_4 are dependent (indicated by $(1, 4) \in \bar{E}$), but they are conditionally independent given the other elements of X (indicated by $(1, 4) \notin E$).

if there is a path $(i, i_1), (i_1, i_2) \dots, (i_q, j) \in E$ that connects i and j (in particular, $E \subset \bar{E}$). For pairwise densities in our framework, it is easy to check that

$$X_i \perp X_j \quad \text{if and only if} \quad (i, j) \notin \bar{E}.$$

Hence, the dependence structure of X is captured by \bar{E} . We give an illustration of these properties in Figure 1.

We can now turn to the examples.

2.2.1 Counting Measure

We first describe two cases where the base measure ν is the counting measure on $\{0, 1, \dots\}^p$. Specifically, we show that the well-known Ising and multinomial Ising models are encompassed by our framework.

Beyond the measure, a unifying property of the two examples is that the integrability condition is satisfied for all matrices. In a formula, this reads

$$\gamma(M) < \infty \quad \text{for all } M \in \mathbb{R}^{p \times p}. \quad (3)$$

Since the set of all matrices in $\mathbb{R}^{p \times p}$ is open, the integrability property (3) means that

$$\mathfrak{M}^* = \{M \in \mathbb{R}^{p \times p}\}.$$

This ensures that any convex and (relatively) open set $\mathfrak{M} \subset \mathbb{R}^{p \times p}$ meets our technical assumptions. Importantly, we show later that the same properties are shared by exponential trace models for Poisson data.

Ising The Ising model has a variety of applications, for example, in Statistical Mechanics and Quantum Field Theory (Gallavotti 2013, Zuber & Itzykson 1977). Its densities are proportional to

$$e^{\sum_{j=1}^p a_{jj}x_j + \sum_{j,k} a_{jk}x_jx_k}$$

with $a_{jk} = a_{kj}$, and the domain is $x_1, \dots, x_p \in \{0, 1\}$. As an illustration, consider a material that consists of p molecules with one “magnetic” electron each. The binary variable x_j then corresponds to the electron’s spin (up or down in a given direction) in the j th molecule, and the factor a_{jk} determines whether the spins of the electrons in the j th and k th molecule tend to align ($a_{jk} > 0$ as in ferromagnetic materials) or tend to take opposite directions ($a_{jk} < 0$ as in anti-ferromagnetic materials). The Ising model is a special case of our framework (2). Indeed, since $1^2 = 1$ and $0^2 = 0$, we can obtain the desired densities by setting $\mathcal{D} = \{0, 1\}^p$, $q = p$, $M_{ij} = -a_{ij}$, $T_{ij}(\mathbf{x}) = x_i x_j$, and $\xi \equiv 0$. Since the domain is finite, the integrability condition $\gamma(M) < \infty$ is naturally satisfied for all matrices M .

Multinomial Ising The spin of spin 1/2 particles (such as the electron) can take two values. Thus, the corresponding measurements can be represented by the domain $\{0, 1\}$ as in the Ising model discussed above. In contrast, the spin of spin s particles with $s \in \{1, 3/2, \dots\}$ (such as W and Z vector bosons and composite particles) can take $2s + 1$ values, which can not be represented by binaries directly. Therefore, the multinomial Ising model, which extends the Ising model to multinomial domains, is of considerable interest in quantum physics. For similar reasons, multinomial Ising models are of interest in other fields, see (Diesner & Carley 2005) for an example in sociology.

We now show that also the multinomial Ising model is a special case of our framework. For this, we encode the data in an enlarged binary vector. We first denote the original multinomial data by $Y \in \{0, \dots, m-1\}^l$. This could correspond to l spin $(m-1)/2$ particles. We then represent the data with an enlarged binary vector $X \in \{0, 1\}^p$, $p = l \cdot (m-1)$, by

setting

$$X_i = \mathbb{1}\left\{Y_j = i - (m-1)\lfloor \frac{i-1}{m-1} \rfloor, j = \lceil \frac{i}{m-1} \rceil\right\} \in \{0, 1\}.$$

Each coordinate of the original data (for example, each spin) is now represented by $m-1$ binary variables. We can use the same model as above, except for imposing the additional requirement $M_{ij} = 0$ if $\lceil \frac{i}{m-1} \rceil = \lceil \frac{j}{m-1} \rceil$ to avoid self-interactions. These settings yield the standard extension of the Ising model to multinomial data, cf. (Loh & Wainwright 2013). In particular, for $m = 2$, we recover the Ising model above. Again, since the domain is finite, the integrability condition $\gamma(M) < \infty$ is naturally satisfied for all matrices M .

2.2.2 Continuous Measure

We now consider two examples in which the base measure ν is the Lebesgue measure on \mathbb{R}^p . Specifically, we show that Gaussian and non-paranormal graphical models are encompassed by our framework.

We show that the integrability condition is satisfied for all matrices that are positive definite. In a formula, this reads

$$\gamma(M) < \infty \text{ for all positive definite } M \in \mathbb{R}^{p \times p}. \quad (4)$$

Since the set of all positive definite matrices in $\mathbb{R}^{p \times p}$ is open, this means that

$$\mathfrak{M}^* \supset \{M \in \mathbb{R}^{p \times p} : M \text{ positive definite}\}.$$

One can thus take any convex and (relatively) open set of positive definite matrices as parameter space \mathfrak{M} . Later, we will show that very similar models can also be formulated for exponential data, for example.

Gaussian The most popular examples are Gaussian graphical models (Lauritzen 1996). For centered data (which can be assumed without loss of generality), these models correspond to random vectors $X \sim \mathcal{N}_p(0, \Sigma)$, where Σ (and thus also Σ^{-1}) is a symmetric, positive definite matrix. We can generate these models in our framework (2) by setting $\mathcal{D} = \mathbb{R}^p$, $q = p$, $M = \Sigma^{-1}$, $T_{ij}(\mathbf{x}) = x_i x_j / 2$, and $\xi \equiv 0$.

Gaussian graphical models are well-studied and are also the starting point for our contribution. It is thus especially important to disentangle general properties of graphical

models in our framework from peculiarities of the Gaussian case. First, the correspondence of the conditional independence structure and the non-zero pattern of the inverse covariance matrix is specific to the Gaussian case. This has already been pointed out in (Loh & Wainwright 2013), where relationships between the dependence structure and the inverse covariance matrix in Ising models and other exponential families with additional interaction terms are studied. However, instead of concentrating on possible connections, we argue that it is important to distinguish clearly between the two concepts. In our framework, the (conditional) dependencies are completely captured by the matrix M . It is thus reasonable to consider M the fundamental quantity. Instead, the equality of M^{-1} and $\mathbb{E}_M[XX^\top]$ is specific to the Gaussian case, and the (generalized) covariances $\mathbb{E}_M[XX^\top]$ ($2\mathbb{E}_M T(X)$) and their inverse should be viewed only as a characteristic of the model. Second, the type of the node conditionals can change once dependencies are introduced. In the Gaussian case, the node conditionals are normal irrespective of M . In most other cases, however, the types of node conditionals cannot be the same in the dependent and independent case - unless additional assumptions are introduced. We will discuss this in the later examples below.

Non-paranormal Well-known generalizations of Gaussian graphical models are non-paranormal graphical models (Liu et al. 2009). These models correspond to vectors X such that

$(g_1(X_1), \dots, g_p(X_p))^\top \sim \mathcal{N}_p(0, \Sigma)$ for real-valued, monotone, and differentiable functions g_1, \dots, g_p and symmetric, positive definite matrix Σ . These models can be generated in our framework by setting $\mathcal{D} = \mathbb{R}^p$, $q = p$, $M = \Sigma^{-1}$, $T_{ij}(\mathbf{x}) = g_i(x_i)g_j(x_j)/2$, and $\xi(\mathbf{x}) = \sum_{j=1}^p \log |g'_j(x_j)|$, cf. (Liu et al. 2009, Equation (2)). The normalization constant is (irrespective of symmetry) $\gamma(M) = \log((2\pi)^p |M^{-1}|)/2 < \infty$ both in the Gaussian and the non-paranormal case, so that in both cases, property (4) is satisfied.

2.3 Non-standard Examples

The idea that Ising models as well as other standard graphical models can be written as exponential families is not new (Wainwright & Jordan 2008, Chapter 3.3). However, we argue that the details of the notions and formulations are essential, especially when it

comes to establishing models for data that are not covered by standard graphical models. We will outline this in the following. We first discuss Poisson and exponential distributions. In particular, we establish thorough proofs for the integrability of the square-root models in (Inouye et al. 2016) and introduce extensions that show that the square-root is just one out of many possible operations for the interaction terms and that a variety of distributions besides Poisson can be handled.

Poisson A main objective in systems biology is the inference of microbial interactions. The corresponding data is multivariate count data with infinite range (Faust et al. 2012). Other fields where such data is prevalent include particle physics (radioactive decay of particles) and criminalistics (number of crimes and arrests). However, copula-based approaches to infinite count data inflict severe identifiability issues (Genest & Nešlehová 2007), while standard extensions of the independent case lead to integrability issues, see below. Multivariate Poisson data has thus obtained considerable attention in the recent Machine Learning literature (Inouye et al. 2016, 2015, Yang et al. 2015, 2013), but much less in statistics.

We show in the following that within framework (2), one can solve the problems associated with the standard approaches while preserving the Poisson flavor of the individual coordinates, especially in the limit of small interactions. For this, we use our framework with the specifications $\mathcal{D} = \{0, 1, \dots\}^p$, $q = p$, $\xi(\mathbf{x}) = -\sum_{j=1}^p \log(x_j!)$, and functions T that satisfy $T_{ii}(\mathbf{x}) = T_{ii}(x_i) = x_i$ and $T_{ij}(\mathbf{x}) = T_{ij}(x_i, x_j) \leq c(x_i + x_j)$ for some $c \in (0, \infty)$. We note that the case $T_{ij}(\mathbf{x}) = \sqrt{x_i x_j}$ has been introduced in the Machine Learning literature (Inouye et al. 2016), but the technical aspects of this case have not been studied, and the general setting has not been formulated altogether.

Most importantly, we need to show property (3). To this end, we have to verify that for all matrices $M \in \mathbb{R}^{p \times p}$

$$\sum_{x_1, \dots, x_p=0}^{\infty} \frac{e^{-\sum_j M_{jj} x_j - \sum_{i,j:i \neq j} M_{ij} T_{ij}(x_i, x_j)}}{\prod_j x_j!} < \infty.$$

Since $-M_{ij} T_{ij}(x_i, x_j) \leq \tilde{c} x_i + \tilde{c} x_j$, where $\tilde{c} := c \max_{i,j} |M_{ij}|$, a sufficient condition is

$$\sum_{x_1, \dots, x_p=0}^{\infty} \frac{e^{-\sum_j (M_{jj} - 2p\tilde{c}) x_j}}{\prod_j x_j!} < \infty.$$

Hence, defining $C(M, j) := e^{-(M_{jj}-2p\bar{c})} \in (0, \infty)$, $j \in \{1, \dots, p\}$, the integrability condition is implied for any M by the fact

$$\sum_{x_1, \dots, x_p=0}^{\infty} \prod_{j=1}^p \frac{C(M, j)^{x_j}}{x_j!} = \prod_{j=1}^p e^{C(M, j)} < \infty.$$

This proves property (3).

In contrast, the corresponding integrability conditions in standard approaches to this data type inflict severe restrictions on the parameter space. To see this, recall that the joint density of p independent Poisson random variables with parameters $a_1, \dots, a_p > 0$ is proportional to

$$\exp\left(\sum_{j=1}^p \log(a_j)x_j - \sum_{j=1}^p \log(x_j!)\right).$$

The standard approach to include interactions is to add terms of the form $a_{ij}x_i x_j$. This yields densities proportional to

$$\exp\left(\sum_{j=1}^p \log(a_j)x_j + \sum_{i \neq j} a_{ij}x_i x_j - \sum_{j=1}^p \log(x_j!)\right). \quad (5)$$

The dominating terms in this expression are the interaction terms $a_{ij}x_i x_j$. Using Stirling's approximation, we find that $x^2/\log(x!) \rightarrow \infty$ for $x \rightarrow \infty$, showing that the density cannot be normalized unless $a_{ij} \leq 0$ for all i, j . This means that the standard approach excludes positive interactions between the nodes.

Let us finally look at the node conditionals for a specific T . We choose $T_{ij}(\mathbf{x}) = \sqrt{x_i x_j}$ for simplicity. The node conditionals become

$$f_M(x_j | \mathbf{x}_{-j}) \sim e^{-M_{jj}x_j - \log(x_j!)} L_{\text{Int}},$$

where

$$L_{\text{Int}} = e^{-\sqrt{x_j} \sum_{k \in \mathcal{N}(j)} (M_{jk} + M_{kj}) \sqrt{x_k}}.$$

The off-diagonal terms in M model the interactions of j with the other nodes. If the factors M_{jk} are small, $L_{\text{Int}} \approx 1$, and thus, the node j approximately follows a Poisson distribution with parameter $e^{-M_{jj}}$. In particular, if M is diagonal, the nodes are independent Poisson distributed random variables.

In comparison, the standard approach represented by Display (5) results in exact Poisson node conditionals for any non-positive correlations. Conversely, it has been shown in (Chen et al. 2015, Proposition 1 and Lemma 1) that one can find a distribution with Poisson (or exponential) node conditionals *only* if all interactions are non-positive. Thus, an unavoidable price for “pure” node conditionals is a strong, in practice typically unrealistic assumption on the parameter space. Our framework avoids this assumption and is still close to the exact Poisson (exponential) distributions if the interactions are small.

Exponential The exponential case is the counterpart of the Poisson case discussed above. In particular, the standard approach to correlated exponential data is confronted with the same integrability issues as above, while approaches via framework (2) easily satisfy the integrability conditions.

To model exponential data, we consider $\mathcal{D} = [0, \infty)^p$, $q = p$, and $\xi \equiv 0$. Again a number of transformations T would have the desired properties; however, to avoid digression, we only consider the square-root transformations $T_{ij}(\mathbf{x}) = \sqrt{x_i x_j}$ that correspond to (Inouye et al. 2016); generalization are possible along the same lines as in the Poisson case. We can now check the integrability condition (4). Denoting the smallest ℓ_2 -eigenvalue of M by $\kappa(M) > 0$, we find

$$\begin{aligned} e^{\gamma(M)} &= \int_0^\infty \dots \int_0^\infty e^{-\sum_{i,j=1}^p M_{ij} \sqrt{x_i x_j}} dx_1 \dots dx_p \\ &\leq \int_0^\infty \dots \int_0^\infty e^{-\kappa(M) \|\mathbf{x}\|_1} dx_1 \dots dx_p \\ &= \left(\int_0^\infty e^{-\kappa(M)x} dx \right)^p \\ &= \kappa(M)^{-p} < \infty. \end{aligned}$$

Hence, $\gamma(M) < \infty$ for all positive definite matrices M .

In contrast, adding linear interaction terms to the independent joint density forbids positive correlations. One can check this similarly as in the Poisson case above.

The node conditionals finally become

$$f_M(x_j | \mathbf{x}_{-j}) \sim e^{-M_{jj}x_j} L_{\text{Int}},$$

where

$$L_{\text{Int}} = e^{-\sqrt{x_j} \sum_{k \in \mathcal{N}(j)} (M_{jk} + M_{kj}) \sqrt{x_k}}.$$

The off-diagonal terms in M model the interactions of j with the other nodes. If the factors M_{jk} are small, $L_{\text{Int}} \approx 1$, and thus, node j approximately follows an exponential distribution with parameter M_{jj} . In particular, if M is diagonal, all node conditionals follow independent exponential distributions.

Composite Models As an example for composite models, let us consider data with Poisson and exponential elements. Note first that the conditions on the set of matrices \mathfrak{M} are different in the discrete examples and the continuous examples: In the discrete examples, we have shown $\gamma(M) < \infty$ for any matrix M . In the continuous examples, we have shown $\gamma(M) < \infty$ under the additional assumption that M is positive definite. In the case of composite models, one can interpolate the conditions. However, for the sake of simplicity, we instead assume that the matrices M are positive definite. We then consider $p_1, p_2 \in \{1, 2, \dots\}$, $p_1 + p_2 = p$, $\mathcal{D} = \{0, 1, \dots\}^{p_1} \times [0, \infty)^{p_2}$, $\mathfrak{M} \subset \{M \in \mathbb{R}^{p \times p} : M \text{ symmetric, positive definite}\}$, \mathfrak{M} open and convex, and $\xi(\mathbf{x}) = -\sum_{j=1}^{p_1} \log(x_j!)$. Hence, the first p_1 elements of the random vector X are discrete, while the other p_2 elements are continuous. Using again the square-root transformation, the Poisson-type node conditionals for $j \in \{1, \dots, p_1\}$ are

$$f_M(x_j | \mathbf{x}_{-j}) \sim e^{-M_{jj}x_j - \log(x_j!)} L_{\text{Int}},$$

where

$$L_{\text{Int}} = e^{-\sqrt{x_j} \sum_{k \in \mathcal{N}(j)} (M_{jk} + M_{kj}) \sqrt{x_k}}.$$

The exponential-type node conditionals for $j \in \{p_1 + 1, \dots, p_1 + p_2\}$ have the corresponding form. The expressions highlight that the densities can include interactions between the discrete and continuous elements of X , while the Poisson/exponential-flavors of the nodes are still preserved.

To show that $\gamma(M) < \infty$, we proceed similarly as in the examples above. More precisely,

denoting the smallest ℓ_2 -eigenvalue of M by $\kappa(M) > 0$, we find

$$\begin{aligned}
e^{\gamma(M)} &= \sum_{x_1, \dots, x_{p_1}=0}^{\infty} \int_0^{\infty} \cdots \int_0^{\infty} \frac{e^{-\sum_{i,j=1}^p M_{ij} \sqrt{x_i x_j}}}{\prod_{j=1}^{p_1} x_j!} dx_{p_1+1} \cdots dx_p \\
&\leq \sum_{x_1, \dots, x_{p_1}=0}^{\infty} \int_0^{\infty} \cdots \int_0^{\infty} \frac{e^{-\kappa(M) \|\mathbf{x}\|_1}}{\prod_{j=1}^{p_1} x_j!} dx_{p_1+1} \cdots dx_p \\
&= \sum_{x_1, \dots, x_{p_1}=0}^{\infty} \frac{e^{-\kappa(M)(x_1 + \cdots + x_{p_1})}}{\prod_{j=1}^{p_1} x_j!} \\
&\quad \times \int_0^{\infty} \cdots \int_0^{\infty} e^{-\kappa(M)(x_{p_1+1} + \cdots + x_{p_2})} dx_{p_1+1} \cdots dx_p \\
&= \left(e^{e^{-\kappa(M)}} \right)^{p_1} \left(\int_0^{\infty} e^{-\kappa(M)x} dx \right)^{p_2} < \infty.
\end{aligned}$$

Laplace and Beyond There is much room for our creativity in constructing models. For example, we can readily establish models for Laplace (double-exponential) data by inserting absolute values throughout, for example, $T_{ij}(\mathbf{x}) = \sqrt{|x_i x_j|}$. Indeed, again denoting the smallest ℓ_2 -eigenvalue of M by $\kappa(M) > 0$, we find

$$\begin{aligned}
e^{\gamma(M)} &= \int_{-\infty}^{\infty} \cdots \int_{-\infty}^{\infty} e^{-\sum_{i,j=1}^p M_{ij} \sqrt{|x_i x_j|}} dx_1 \cdots dx_p \\
&\leq \int_{-\infty}^{\infty} \cdots \int_{-\infty}^{\infty} e^{-\kappa(M) \|\mathbf{x}\|_1} dx_1 \cdots dx_p \\
&= \left(2 \int_0^{\infty} e^{-\kappa(M)x} dx \right)^p \\
&= (2/\kappa(M))^p < \infty.
\end{aligned}$$

Hence, $\gamma(M) < \infty$ for all positive definite matrices M . In general, the essentially only limit is that to ensure integrability, the interaction terms have to be of “smaller order” than the terms that correspond to the independent case.

3 Estimation

We now turn to estimation based on maximum likelihood. In Section 3.1, we show that maximum likelihood estimation has desirable properties in our framework. In Section 3.2, we propose a sampling-based approximation algorithm for computing the maximum likelihood estimator.

3.1 Maximum Likelihood Estimation

We study maximum likelihood estimation in our framework. For this, we assume we are given n i.i.d. data samples X^1, \dots, X^n from a distribution of the form (2). Also, we assume we are given the model specifications \mathcal{D}, ν, T, ξ and the parameter space \mathfrak{M} ; that is, we assume that the model class is known. In contrast, the correct model parameters specified in the matrix M are unknown. Our goal is to estimate M from the data.

As a toy example, consider data on p different populations of freshwater fish in n similar lakes. More specifically, consider vector-valued observations $X^1, \dots, X^n \in \{0, 1, \dots\}^p$, where $(X^i)_j$ is the number of fish of type j in lake i . We want to use these data to uncover the relationships among the different populations. A model suited for this task is the Poisson model discussed earlier. For example, we might set $\mathcal{D} = \{0, 1, \dots\}^p$, $q = p$, $\{M \in \mathbb{R}^{p \times p} : M \text{ symmetric}\}$, $T_{ij}(\mathbf{x}) = \sqrt{x_i x_j}$, and $\xi(\mathbf{x}) = -\sum_{j=1}^p \log(x_j!)$. The relationships among the fish populations are then encoded in M , which then needs to be estimated from the observations.

Before heading on, we add some convenient notation. We summarize the data in $\underline{X} := (X^1, \dots, X^n)$ and denote the corresponding function argument by $\underline{\mathbf{x}} := (\mathbf{x}^1, \dots, \mathbf{x}^n)$ for $\mathbf{x}^1, \dots, \mathbf{x}^n \in \mathcal{D}$. The generalized Gram matrix is denoted by

$$\bar{T}(\underline{\mathbf{x}}) := \frac{1}{n} \sum_{i=1}^n T(\mathbf{x}^i).$$

The negative joint log-likelihood function $-\ell_M$ for n i.i.d random vectors corresponding to the model (2) is finally given by

$$-\ell_M(\underline{\mathbf{x}}) = n \langle M, \bar{T}(\underline{\mathbf{x}}) \rangle_{\text{tr}} - \sum_{i=1}^n \xi(\mathbf{x}^i) + n\gamma(M).$$

We can now state the maximum likelihood estimator and its properties. For further reference, we first state the essence of the previous discussion in the following lemma.

Lemma 3.1 (Log-likelihood). *Given any $M \in \mathfrak{M}^*$, the negative joint log-likelihood function $-\ell_M$ of n i.i.d. random vectors distributed according to f_M in (2) can be expressed by*

$$-\ell_M(\underline{\mathbf{x}}) = n \langle M, \bar{T}(\underline{\mathbf{x}}) \rangle_{\text{tr}} + n\gamma(M) + c,$$

where $c \in \mathbb{R}$ does not depend on M .

Motivated by Lemma 3.1, we introduce the maximum likelihood estimator of M by

$$\widehat{M} := \operatorname{argmin}_{\widetilde{M} \in \mathfrak{M}} \{ -\ell_{\widetilde{M}}(\underline{X}) \} = \operatorname{argmin}_{\widetilde{M} \in \mathfrak{M}} \{ \langle \widetilde{M}, \overline{T}(\underline{X}) \rangle_{\text{tr}} + \gamma(\widetilde{M}) \}. \quad (6)$$

The estimator exists in all generic examples. More generally, under our assumption that $M \in \mathfrak{M} \subset \mathfrak{M}^*$ and \mathfrak{M} is open and convex, and the minimizer exists for n sufficiently large, cf. (Berk 1972). In particular, the objective function is convex, and its derivatives can be computed explicitly.

Lemma 3.2 (Convexity). *For any $\underline{x} \in \mathcal{D}^p$, the function*

$$\begin{aligned} \mathfrak{M}^* &\rightarrow \mathbb{R} \\ M &\mapsto \langle M, \overline{T}(\underline{x}) \rangle_{\text{tr}} + \gamma(M) \end{aligned}$$

is convex.

Lemma 3.3 (Derivatives). *For any $\underline{x} \in \mathcal{D}^p$, the function*

$$\begin{aligned} \mathfrak{M}^* &\rightarrow \mathbb{R} \\ M &\mapsto \langle M, \overline{T}(\underline{x}) \rangle_{\text{tr}} + \gamma(M) \end{aligned}$$

is twice differentiable with partial derivatives

$$\frac{\partial}{\partial M_{ij}} (\langle M, \overline{T}(\underline{x}) \rangle_{\text{tr}} + \gamma(M)) = \overline{T}_{ij}(\underline{x}) - \mathbb{E}_M \overline{T}_{ij}(\underline{X})$$

and

$$\begin{aligned} \frac{\partial}{\partial M_{ij}} \frac{\partial}{\partial M_{kl}} (\langle M, \overline{T}(\underline{x}) \rangle_{\text{tr}} + \gamma(M)) \\ = n \mathbb{E}_M [(\overline{T}_{ij}(\underline{X}) - \mathbb{E}_M \overline{T}_{ij}(\underline{X}))(\overline{T}_{kl}(\underline{X}) - \mathbb{E}_M \overline{T}_{kl}(\underline{X}))] \end{aligned}$$

for $i, j, k, l \in \{1, \dots, q\}$.

Convexity and the explicit derivatives are desirable for both optimization and theory. From an optimization perspective, the two properties are valuable, because they render the objective function amenable to gradient-type minimization. From a theoretical perspective, the two properties are valuable, because they imply that

$$M = \operatorname{argmin}_{\widetilde{M} \in \mathfrak{M}} \{ \mathbb{E}_M [\langle \widetilde{M}, \overline{T}(\underline{X}) \rangle_{\text{tr}} + \gamma(\widetilde{M})] \},$$

showing that $\widehat{\mathbb{M}}$ is a standard M-estimator, and because they imply that $\widehat{\mathbb{M}}$ can be written as a Z-estimator (note that $\widehat{\mathbb{M}}$ is necessarily in the interior of \mathfrak{M}) with criterion

$$\overline{T}(\underline{X}) = \mathbb{E}_{\widehat{\mathbb{M}}} \overline{T}(\underline{X}).$$

A simple special case is the multivariate Gaussian model. Recall that in this case, \mathbb{M} is the inverse of the usual population covariance matrix. Moreover, one can check that

$$\overline{T}(\underline{\mathbf{x}}) = \frac{1}{n} \sum_{i=1}^n \mathbf{x}^i \mathbf{x}^{i\top}$$

and $\widehat{\mathbb{M}} = \overline{T}(\underline{X})^{-1}$. Hence, in this case, the estimator $\widehat{\mathbb{M}}$ is the inverse of the (usual) sample covariance matrix.

Remark 3.1. *The maximum likelihood estimator of \mathbb{M} is asymptotically normal with covariance equal to the inverse Fisher information. In particular, consistency and asymptotic normality of the maximum likelihood estimator can be proved following the arguments in the classical paper (Berk 1972), see especially (Berk 1972, Theorems 4.1 and 6.1). We refer to that paper for details.*

3.2 Algorithm

The main challenge in computing the maximum likelihood estimator is the unconventional normalization term. We address this challenge by approximating the objective function using a sampling-based technique. In this section, we describe the corresponding algorithm.

We denote the objective function of the maximum likelihood estimator in Equation (6) as

$$g(\widetilde{\mathbb{M}}) := \langle \widetilde{\mathbb{M}}, \overline{T}(\underline{X}) \rangle_{\text{tr}} + \gamma(\widetilde{\mathbb{M}}).$$

The normalization term $\gamma(\widetilde{\mathbb{M}})$, in general, does not have a closed-form formula and, therefore, makes the objective function hard to compute exactly. However, we show in the following that it can be feasibly approximated. Adding the constant term $\gamma(\mathbb{M}_0)$, where \mathbb{M}_0 is a pre-specified constant parameter matrix, to the objective function of (6) yields an equivalent definition of the maximum likelihood estimator as

$$\widehat{\mathbb{M}} = \underset{\widetilde{\mathbb{M}} \in \mathfrak{M}}{\operatorname{argmin}} \{ \langle \widetilde{\mathbb{M}}, \overline{T}(\underline{X}) \rangle_{\text{tr}} + \gamma(\widetilde{\mathbb{M}}) - \gamma(\mathbb{M}_0) \}. \quad (7)$$

Algebraic transformation reveals

$$\gamma(\tilde{M}) - \gamma(M_0) = \log \mathbb{E}_{M_0} \left(e^{-\langle \tilde{M} - M_0, T(\mathbf{x}) \rangle_{\text{tr}}} \right).$$

The finite expectation can be approximated by an empirical mean based on some sample set Y from the distribution $f_{M_0}(\mathbf{x}) := \exp(-\langle M_0, T(\mathbf{x}) \rangle_{\text{tr}} + \xi(\mathbf{x}) - \gamma(M_0))$. By the strong law of large numbers, when the cardinality of the set Y (denoted as $|Y|$) goes to infinity, the empirical mean approximates the expectation well:

$$\log \frac{1}{|Y|} \sum_{Z \in Y} e^{-\langle M - M_0, T(Z) \rangle_{\text{tr}}} \xrightarrow{a.s.} \log \mathbb{E}_{M_0} \left(e^{-\langle M - M_0, T(\mathbf{x}) \rangle_{\text{tr}}} \right).$$

Hence, in practice, we solve the approximate problem

$$\hat{M} \approx \underset{\tilde{M} \in \mathfrak{M}}{\text{argmin}} \{ \tilde{g}(\tilde{M}) \}, \quad (8)$$

where

$$\tilde{g}(\tilde{M}) := \langle \tilde{M}, \bar{T}(\underline{X}) \rangle_{\text{tr}} + \log \frac{1}{|Y|} \sum_{Z \in Y} e^{-\langle \tilde{M} - M_0, T(Z) \rangle_{\text{tr}}}.$$

We apply gradient descent to solve the problem of (8). The gradient with respect to \tilde{M} is

$$\nabla \tilde{g}(\tilde{M}) = \bar{T}(\underline{X}) - \frac{\sum_{Z \in Y} T(Z) e^{-\langle \tilde{M} - M_0, T(Z) \rangle_{\text{tr}}}}{\sum_{Z \in Y} e^{-\langle \tilde{M} - M_0, T(Z) \rangle_{\text{tr}}}}. \quad (9)$$

Remark 3.2. *The gradient in (9) can also be considered as an instantiation of self-normalized importance sampling (Owen 2013). Lemma 3.3 gives the gradient of $g(\tilde{M})$ in the form of*

$$\nabla g(\tilde{M}) = \bar{T}(\underline{X}) - \mathbb{E}_{\tilde{M}} \bar{T}(\underline{X}) = \bar{T}(\underline{X}) - \mathbb{E}_{\tilde{M}} T(X).$$

When $\mathbb{E}_{\tilde{M}} T(X)$ lacks an algebraic expression and $f_{\tilde{M}}$ is inconvenient to sample from, importance sampling (Owen 2013) is useful to approximate the expectation term $\mathbb{E}_{\tilde{M}} T(X)$. The idea of importance sampling is to draw samples from a biased distribution and obtain the desired $f_{\tilde{M}}$ by adjusting the weights for the drawn samples. Self-normalized importance sampling refers to the special case when weights are normalized by their sum. Equation (9) reflects the same idea and uses the pre-specified f_{M_0} as the biased sampling distribution.

The choice of M_0 is essential for the finite-sample performance of the approximation. Our two main considerations are: First, the sampling distribution f_{M_0} should be straightforward for generating samples. Second, it should lead to balanced weights and a small

variance of $\widehat{\mathbb{E}}_{\widetilde{\mathbf{M}}}T(X)$; if weights concentrate in just a few samples, we have effectively only got these observations, resulting in large variability of the approximation (Owen 2013). To incorporate the two considerations, we propose

$$M_0 := \operatorname{argmin}_{\widetilde{\mathbf{M}} \in \mathfrak{M}} \{ \langle \widetilde{\mathbf{M}}, \overline{T(\underline{X})} \rangle_{\text{tr}} + \gamma(\widetilde{\mathbf{M}}) \} \quad \text{subject to } \widetilde{M}_{kl} = 0, \quad \forall k \neq l. \quad (10)$$

We restrict the parameter to a diagonal matrix, by which we presume mutual independence among all coordinates and disentangle the objective function. Hence, both the optimizing problem (10) and the task of sampling from f_{M_0} can be handled for each coordinate separately, and each coordinate reduces to a standard univariate exponential family distribution. Besides, M_0 is the diagonal matrix closest to the actual parameter. When the off-diagonal entries of the actual parameter matrix are small, weights of the drawn samples are expected to be reasonable.

Algorithm 1 summarizes our computational pipeline. In the full version, which is stated in Appendix B, a backtracking line search selects the step size adaptively and incorporates the domain constraint as needed (for example, the positive definite requirement for the case of continuous measures).

4 Simulation Studies

Exponential trace models apply to a large variety of multivariate data that have correlated coordinates. The framework is especially useful for data that are discrete, heavy-tailed, or composed of different data types. We consider the following four model-types in simulations: Poisson, Exponential, Poisson-Bernoulli (a composite of Poisson and Bernoulli), and Poisson-Gaussian (a composite of Poisson and Gaussian). Such types of models are useful in practice but, to date, have proven challenging to characterize and estimate.

4.1 Settings

We follow the discussion of Section 2.3 and consider the square-root transformation for non-Gaussian data as one example, that is, we set $T_{ij}(\mathbf{x}) = t_i(x_i)t_j(x_j)$, where $t_i(x_i) = \sqrt{x_i}$ for non-Gaussian coordinates and $t_i(x_i) = x_i$ for Gaussian coordinates.

Algorithm 1: Solving for the maximum likelihood estimator

```
//  $\eta$ : step size
Input :  $\bar{T}(\underline{X}), \eta > 0$ 
Output:  $\hat{M}$ 
// Solve for  $M_0$ 
1  $M_0 \leftarrow \mathbf{0}_{p \times p}$ ;
2 for  $i = 1, \dots, p$  do
3    $(M_0)_{ii} \leftarrow \operatorname{argmin}_{m \in \mathbb{R}} \left\{ m \bar{T}_{ii}(\underline{X}) + \log \int \exp(-m T_{ii}(\mathbf{x}) + \xi(x_i)) dx_i \right\}$ ;
   // Generate sample set  $Y$  from  $f_{M_0} = \prod_{i=1}^p f_{(M_0)_{ii}}(x_i)$ 
4 for  $i = 1, \dots, p$  do
5    $\left[ \right.$  Generate 10,000 random samples from  $f_{(M_0)_{ii}}(x_i)$  for the  $i$ -th coordinate;
   // Apply gradient descent with constant step size to (8)
6  $k \leftarrow 0$ ;
7  $\tilde{M}_k \leftarrow M_0$ ;
8 repeat
9    $k \leftarrow k + 1$ ;
10   $\nabla \tilde{g}(\tilde{M}_{k-1}) \leftarrow \bar{T}(\underline{X}) - \frac{\sum_{Z \in Y} T(Z) e^{-(\tilde{M}_{k-1} - M_0, T(Z))_{\text{tr}}}}{\sum_{Z \in Y} e^{-(\tilde{M}_{k-1} - M_0, T(Z))_{\text{tr}}}}$ ;
11   $\tilde{M}_k \leftarrow \tilde{M}_{k-1} - \eta \nabla \tilde{g}(\tilde{M}_{k-1})$ ;
12 until  $|\tilde{g}(\tilde{M}_k) - \tilde{g}(\tilde{M}_{k-1})| < 10^{-4}$ ;
13  $\hat{M} \leftarrow \tilde{M}_k$ ;
```

In the following, we describe the specific graph structures for discrete data, continuous data, and composite data of both types. The discrete data category also covers composite data of different discrete types (for example, Poisson-Bernoulli).

Discrete Data

We consider Erdős-Rényi random graphs and generate the corresponding $p \times p$ parameter matrix M in the following manner. Let c_0 and c_1 be two constants ($c_1 \neq 0$). We set the diagonal entries to $M_{ii} = c_0$. For $i \neq j$, the off-diagonal entries are independent and identically distributed as

$$M_{ij} = M_{ji} = \begin{cases} c_1 & \text{with probability } 1/p, \\ -c_1 & \text{with probability } 1/p, \\ 0 & \text{with probability } 1 - 2/p. \end{cases} \quad (11)$$

The corresponding Erdős-Rényi random graph has $p - 1$ edges in expectation, among which half represent positive interactions and the other half negative ones.

Continuous Data

We consider again Erdős-Rényi random graphs. In addition, we generate strictly diagonally dominant matrices with positive diagonal entries for the parameter matrix M . It can be shown that the M 's are positive definite and satisfy the integrability condition. More specifically, we first generate a $p \times p$ adjacency matrix with i.i.d. off-diagonal entries

$$A_{ij} = A_{ji} = \begin{cases} 1 & \text{with probability } 1/p, \\ -1 & \text{with probability } 1/p, \\ 0 & \text{with probability } 1 - 2/p, \end{cases}$$

We denote the maximum node degree by $s := \max_i \sum_{j \neq i} |A_{ij}|$. Then, a positive definite M can be generated by setting the diagonal entries to 1 and the off-diagonal entries to

$$M_{ij} = M_{ji} = 1/(s + 0.1)A_{ij}.$$

The corresponding Erdős-Rényi random graph has $p - 1$ edges in expectation, among which half represent positive interactions and the other half negative ones.

A Composite of Discrete and Continuous Data

We consider even values of p , with the first $p_1 = p/2$ coordinates discrete, and the remaining $p_2 = p/2$ coordinates continuous. The parameter matrix in blockwise format is

$$M = \begin{bmatrix} M_{11} & M_{12} \\ M_{12}^\top & M_{22} \end{bmatrix},$$

where M_{11}, M_{22} represent the conditional dependences among p_1 discrete and p_2 continuous coordinates, respectively. The remaining block M_{12} describes the conditional dependences between discrete and continuous coordinates. When the continuous node conditionals follow a Gaussian distribution, the integrability condition is satisfied for all $M \in \mathbb{R}^{p \times p}$ such that M_{22} is positive definite. Therefore, we generate M_{22} in the above described continuous case to guarantee its positive definiteness while generating M_{11} and M_{12} in the above described discrete case.

4.2 Results

We evaluate the maximum likelihood estimators in terms of edge recovery by studying average ROC (receiver operating characteristic) curves based on thresholding maximum likelihood estimates. Each average ROC curve is taken over 50 individual ROC curves that correspond to 50 different Erdős-Rényi random graphs. ROC curves are combined using horizontal-averaging via the R package `ROCR` (Sing et al. 2005). Since Gaussian graphical models are currently widely used, even in cases with obvious misspecification (eg. count data) (Zhao & Duan 2019), we compare the maximum likelihood estimators of the exponential trace model to that of the (misspecified) Gaussian graphical model.

The graph structures are described in Section 4.1. Details regarding the data generation approaches are deferred to Appendix C. We use $n = 250$ independent observations to recover the conditional dependence of $p = 20$ variables. The diagonal entry is $c_0 = -1$ and the off-diagonal entry is $c_1 = 0.3$. We show the average ROC curves of Poisson, Exponential, Poisson-Bernoulli, and Poisson-Gaussian in Figures 2 and 4. In addition, we explore scenarios with diagonal entry $c_0 \in \{0, -0.5, -1, -1.5, -2\}$ and off-diagonal entry

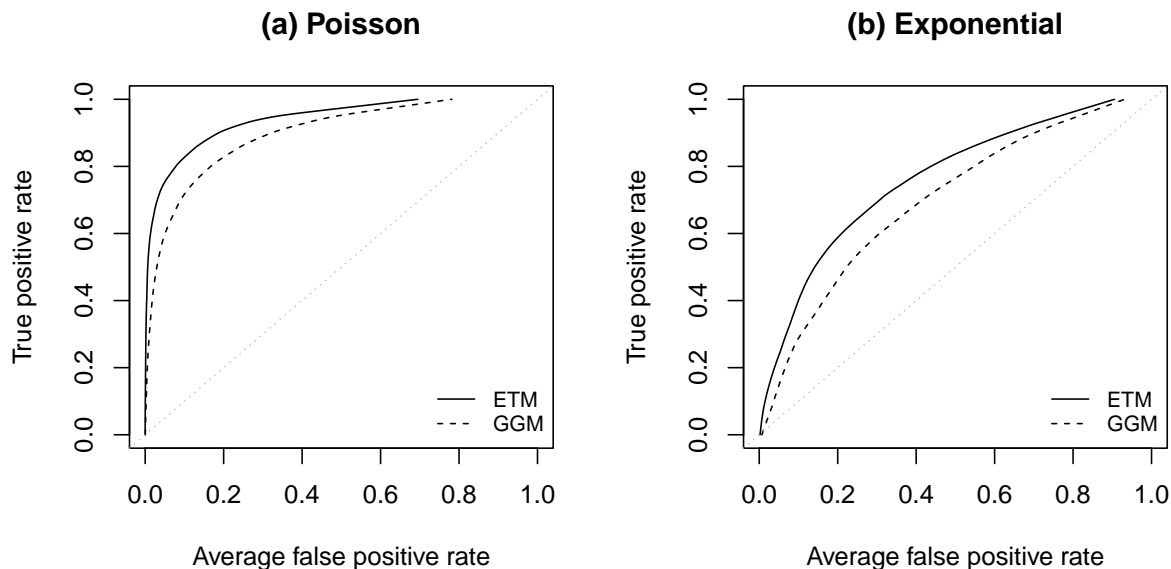


Figure 2: Average ROC curves for pure data. ETM stands for the Exponential trace mode and GGM stands for Gaussian graphical model.

$c_1 \in \{0.1, 0.2, 0.3, 0.4, 0.5\}$: we show the differences in AUC of average ROC curves between the exponential trace model and the Gaussian graphical model in Figures 3 and 5.

In the pure data type scenarios: The exponential trace model outperforms the Gaussian graphical model substantially—the exponential trace model’s ROC curves lie entirely above the Gaussian graphical model’s ROC curves—in the scenario of small interaction and small sufficient statistics $T(\mathbf{x})$ (see Figure 2). In addition, we look into more configurations of Poisson type scenarios by varying c_0 and c_1 : the performance of the sampling-based approximation determines that of the exponential trace model (see Figure 3). When the interaction term and sufficient statistics are small to moderate, the exponential trace model has a larger AUC than the Gaussian graphical model. But when the interaction term and sufficient statistics are large, for example, $c_0 = -2$ and $c_1 = 0.5$, the improvement is not guaranteed. For the composite data type scenarios: The exponential trace model shows improved performance for Poisson-Bernoulli data but not for Poisson-Gaussian data (see Figures 4 and 5). Bernoulli data have very small sufficient statistics so that the improve-

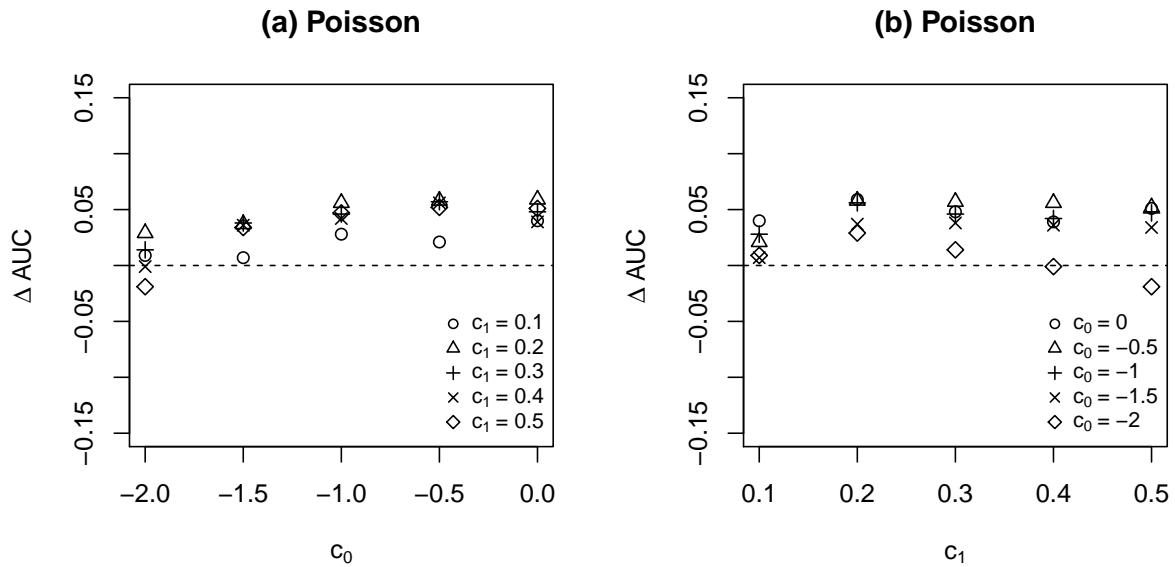


Figure 3: Differences in AUC of average ROC curve between exponential trace model and Gaussian graphical model for Poisson data.

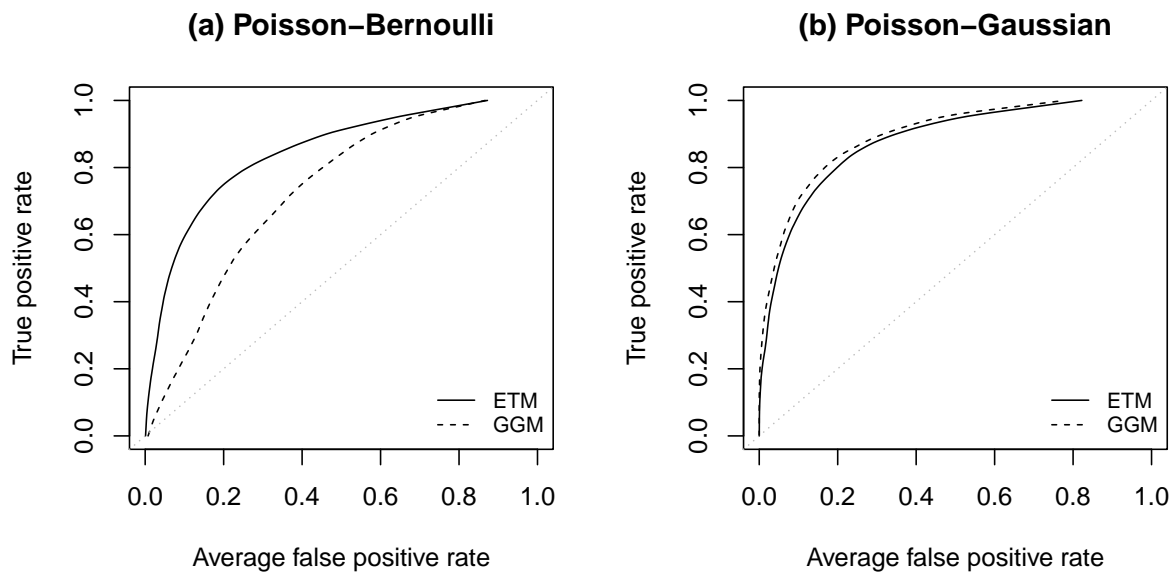


Figure 4: Average ROC curves for composite data. ETM stands for the Exponential trace mode and GGM stands for Gaussian graphical model.

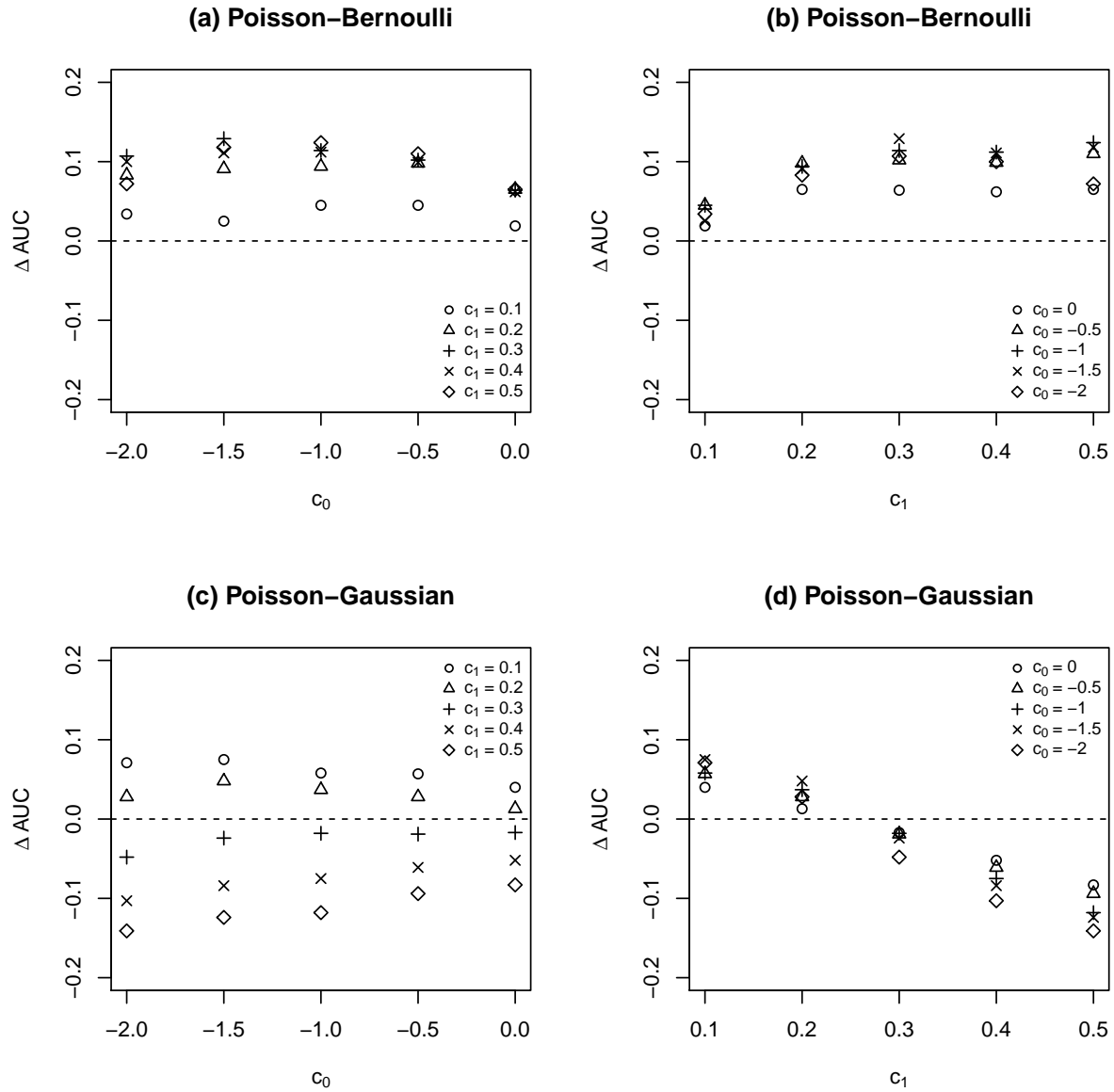


Figure 5: Differences in AUC of average ROC curves between exponential trace model and Gaussian graphical model for composite data.

ment in Poisson-Bernoulli data is substantial for a large range of interaction terms, but Poisson-Gaussian data involves Gaussian coordinates, so that the performance of the exponential trace model is mixed. The comparative performance is not only determined by the performance of the approximation algorithm but also the degree to which the conditional dependence structure resembles the zero pattern of the precision matrix.

In conclusion, the simulation study shows that: (1) the exponential trace model can improve on the Gaussian graphical model for non-Gaussian data, especially when the sufficient statistics and small interactions are small; (2) the approximation approach can struggle when sufficient statistics and interactions are large. Based on this, we believe that our modeling approach has substantial potential: Some of this potential is realized by our current implementation, however some of the potential might require additional computational insights.

5 Application to Neural Spike Data

In this section, we apply the proposed exponential trace model to neural spike data. The temporal and spatial patterns of neural spikes capture the concurrent activity of neurons. Understand this is essential for learning neural circuits. Neural spike data is usually formulated as spike counts in a short time bin and modeled by a Poisson distribution (Theis et al. 2016). We consider a data set of multi-electrode array recordings of spike trains in mouse retina (Demas et al. 2003) obtained from the Retinal Wave Repository (*Home page for the Retinal Wave Repository* 2014). We transform the spike time data into spike counts in time bins of 40 ms following conventions in neural science (Theis et al. 2016). The short time interval captures the instantaneous characteristics of neuron firing. The recording covers an $800 \times 800\ \mu\text{m}$ surface area and provides locations of each recorded unit in the form of (x, y) -coordinates. The number of recorded units ranges from 12 to 22 in different mice.

The spike counts of each recorded unit range from 0 to 13 and roughly follow the mean-variance relationship of a Poisson distribution. The small counts imply: (1) the exponential trace model with square-root transformation is close to the Poisson one; (2) the properties of the data fit the scenario for which the proposed algorithm is appropriate. These two observations render the exponential trace model with a square-root transformation

appropriate.

In Figures 6, we present the recovered connections of recorded units for a 6-week-old wild-type mouse. To obtain sparse graphs, the maximum likelihood estimator is thresholded to 30 edges. In the plotted graphs, the positions of the nodes correspond to [slightly jittered] (x, y) -coordinates of the neurons in the recording. This allows us to consider spatial summaries, eg. the average physical length of edges in our graph.

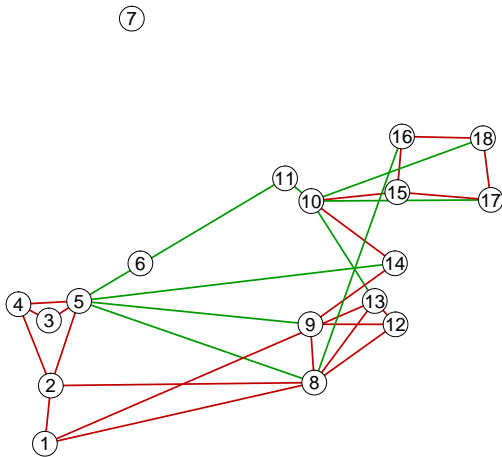
The exponential trace model finds a more centralized graph than the Gaussian graphical model, that is, neurons located together tend to connect in the exponential trace model approach while the estimated connections in the graph are longer in the Gaussian approach. To evaluate this difference quantitatively, we compute the mean Euclidean distance between all pairs of directly connected neurons. In the 6-week-old wild-type mouse, the mean distance is $169 \mu m$ (SE: $24 \mu m$) under the exponential trace model and $252 \mu m$ (SE: $36 \mu m$) under the Gaussian graphical model. In addition, the exponential trace model recovers a main connection component and an isolated neuron unit (see Unit 7 in Figure 6). The isolated neuron unit is physically far away from the primary component and may belong to another functional group. In contrast, the Gaussian graphical model does not distinguish the location separation clearly but instead connects almost every units.

These characteristics found in the exponential trace model but not the Gaussian graphical model align with our biological understanding. In particular, neurons transmit signals to others through synapses, which are physical connections between two neurons (Lodish et al. 2008). This biological mechanism favors direct coordination of closely located neurons. Specifically, previous studies find that the degree two units spike together within some small time window decays with the distance separating the neurons in retina (Cutts & Eglén 2014, Wong et al. 1993, Xu et al. 2011).

6 Discussion

In this paper we proposed an exponential family-based framework to build graphical models. This framework for graphical models allows for a wide range of data types as highlighted in Sections 2.2 and 2.3 and yet ensures a rigid theoretical structure as demonstrated in

ETM



GGM

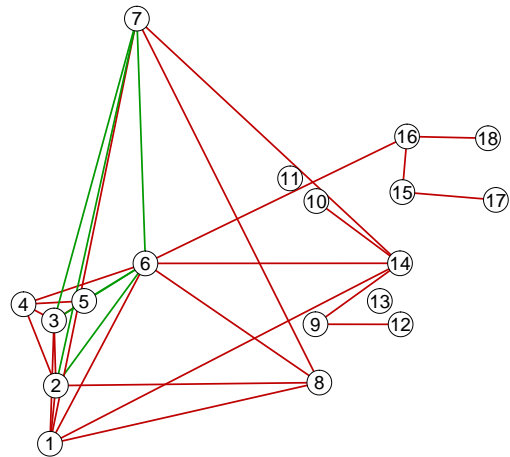


Figure 6: Retinal connections recovered for a 6-week-old wild-type mouse of the Demas et al. 2003 data. The positive interactions are drawn in red, and the negative ones in green. The left panel displays the connection recovered by the exponential model with square-root transformation; the right panel displays the connection recovered by the Gaussian graphical model.

Section 3. The models are amenable to estimation based on maximum likelihood, which can be computed through a sampling-based approximation technique.

Acknowledgements

We also thank Jon Wellner, Marco Rossini, Mathias Drton, Sam Koelle, Zack Almquist, Ali Shojaie, Lina Lin for their valuable input.

References

- Berk, R. H. (1972), ‘Consistency and asymptotic normality of MLE’s for exponential models’, *Ann. Mat. Statist.* **43**, 193–204.
- Besag, J. (1974), ‘Spatial interaction and the statistical analysis of lattice systems’, *J. Roy. Statist. Soc. Ser. B* **36**, 192–236. With discussion by D. R. Cox, A. G. Hawkes, P.

- Clifford, P. Whittle, K. Ord, R. Mead, J. M. Hammersley, and M. S. Bartlett and with a reply by the author.
- Brush, S. G. (1967), ‘History of the Lenz-Ising model’, *Reviews of modern physics* **39**(4), 883.
- Chen, S., Witten, D. M. & Shojaie, A. (2015), ‘Selection and estimation for mixed graphical models’, *Biometrika* **102**(1), 47–64.
- Cutts, C. S. & Eglén, S. J. (2014), ‘Detecting pairwise correlations in spike trains: An objective comparison of methods and application to the study of retinal waves’, *J. Neurosci.* **34**(43), 14288–14303.
- Demas, J., Eglén, S. J. & Wong, R. O. (2003), ‘Developmental loss of synchronous spontaneous activity in the mouse retina is independent of visual experience’, *J. Neurosci.* **23**(7), 2851–2860.
- Diesner, J. & Carley, K. M. (2005), Exploration of communication networks from the enron email corpus, in ‘SIAM International Conference on Data Mining: Workshop on Link Analysis, Counterterrorism and Security, Newport Beach, CA’, Citeseer.
- Drton, M. & Maathuis, M. H. (2016), ‘Structure learning in graphical modeling’, *arXiv:1606.02359* .
- Eaton, M. L. (2007), ‘Multivariate statistics: A vector space approach’, *IMS Lecture Notes Monogr. Ser.* **53**.
URL: <http://projecteuclid.org/euclid.lnms/1196285102>
- Faust, K., Sathirapongsasuti, J. F., Izard, J., Segata, N., Gevers, D., Raes, J. & Huttenhower, C. (2012), ‘Microbial co-occurrence relationships in the human microbiome’, *PLOS Comput. Biol.* **8**(7), e1002606.
- Gallavotti, G. (2013), *Statistical mechanics: A short treatise*, Springer Science & Business Media.

- Genest, C. & Nešlehová, J. (2007), ‘A primer on copulas for count data’, *Astin Bull.* **37**(2), 475–515.
- Grimmett, G. R. (1973), ‘A theorem about random fields’, *Bull. London Math. Soc.* **5**, 81–84.
- Gu, Q., Cao, Y., Ning, Y. & Liu, H. (2015), ‘Local and global inference for high dimensional nonparanormal graphical models’, *arXiv:1502.02347* .
- Home page for the Retinal Wave Repository* (2014), <http://www.damtp.cam.ac.uk/user/eglen/waverepo>.
- Inouye, D. I., Ravikumar, P. & Dhillon, I. S. (2016), ‘Square root graphical models: Multivariate generalizations of univariate exponential families that permit positive dependencies’, *Proceedings of the International Conference on Machine Learning* .
- Inouye, D. I., Ravikumar, P. K. & Dhillon, I. S. (2015), Fixed-length Poisson MRF: adding dependencies to the multinomial, *in* ‘NIPS’, pp. 3195–3203.
- Johansen, S. (1979), *Introduction to the theory of regular exponential families*, Vol. 3 of *Lecture Notes*, University of Copenhagen, Institute of Mathematical Statistics, Copenhagen.
- Lauritzen, S. L. (1996), *Graphical models*, Vol. 17 of *Oxford Statistical Science Series*, The Clarendon Press, Oxford University Press, New York. Oxford Science Publications.
- Lenz, W. (1920), ‘Beiträge zum Verständnis der magnetischen Eigenschaften in festen Körpern’, *Physikalische Zeitschrift* **21**, 613–615.
- Lin, L., Drton, M. & Shojaie, A. (2016), ‘Estimation of high-dimensional graphical models using regularized score matching’, *Electron. J. Stat.* **10**(1), 806.
- Liu, H., Han, F., Yuan, M., Lafferty, J. & Wasserman, L. (2012), ‘High-dimensional semiparametric Gaussian copula graphical models’, *Ann. Statist.* **40**(4), 2293–2326.
- Liu, H., Lafferty, J. & Wasserman, L. (2009), ‘The nonparanormal: semiparametric estimation of high dimensional undirected graphs’, *J. Mach. Learn. Res.* **10**, 2295–2328.

- Lodish, H., Darnell, J. E., Berk, A., Kaiser, C. A., Krieger, M., Scott, M. P., Bretscher, A., Ploegh, H. & Matsudaira, P. (2008), *Molecular cell biology*, Macmillan.
- Loh, P.-L. & Wainwright, M. J. (2013), ‘Structure estimation for discrete graphical models: generalized covariance matrices and their inverses’, *Ann. Statist.* **41**(6), 3022–3049.
- Mahani, A. S. & Sharabiani, M. T. (2014), ‘Multivariate-from-univariate MCMC sampler: R Package MfUSampler’, *arXiv:1412.7784* .
- Neal, R. M. (2003), ‘Slice sampling’, *Ann. Statist.* **31**(3), 705–767.
- Owen, A. B. (2013), *Monte Carlo theory, methods and examples*.
- Shao, J. (2003), *Mathematical statistics*, Springer Texts in Statistics, second edn, Springer-Verlag, New York.
- Sing, T., Sander, O., Beerenwinkel, N. & Lengauer, T. (2005), ‘ROCR: visualizing classifier performance in R’, *Bioinformatics* **21**(20), 3940–3941.
- Theis, L., Berens, P., Froudarakis, E., Reimer, J., Rosón, M. R., Baden, T., Euler, T., Tolias, A. S. & Bethge, M. (2016), ‘Benchmarking spike rate inference in population calcium imaging’, *Neuron* **90**(3), 471–482.
- Wainwright, M. J. & Jordan, M. I. (2008), *Graphical models, exponential families, and variational inference*, Vol. 1, Now Publishers Inc.
- Wong, R. O., Meister, M. & Shatz, C. J. (1993), ‘Transient period of correlated bursting activity during development of the mammalian retina’, *Neuron* **11**(5), 923–938.
- Xu, H.-p., Furman, M., Mineur, Y. S., Chen, H., King, S. L., Zenisek, D., Zhou, Z. J., Butts, D. A., Tian, N., Picciotto, M. R. & Crair, M. C. (2011), ‘An instructive role for patterned spontaneous retinal activity in mouse visual map development’, *Neuron* **70**(6), 1115–1127.
- Xue, L. & Zou, H. (2012), ‘Regularized rank-based estimation of high-dimensional non-paranormal graphical models’, *Ann. Statist.* **40**(5), 2541–2571.

- Yang, E., Ravikumar, P., Allen, G. I. & Liu, Z. (2015), ‘On graphical models via univariate exponential family distributions’, *J. Mach. Learn. Res.* **16**, 3813–3847.
- Yang, E., Ravikumar, P. K., Allen, G. I. & Liu, Z. (2013), On Poisson graphical models, *in* ‘NIPS’, pp. 1718–1726.
- Yu, S., Drton, M. & Shojaie, A. (2019), ‘Generalized score matching for non-negative data.’, *J. Mach. Learn. Res.* **20**(76), 1–70.
- Zhao, H. & Duan, Z.-H. (2019), ‘Cancer genetic network inference using Gaussian graphical models’, *Bioinform. Biol. Insights* **13**, 1–9.
- Zuber, J.-B. & Itzykson, C. (1977), ‘Quantum field theory and the two-dimensional Ising model’, *Physical Review D* **15**(10), 2875.

A Proofs

A.1 Proof of Lemma 2.1

Proof of Lemma 2.1. We prove the two properties in order. The main proof ideas can also be found in (Berk 1972, Pages 193-195).

Property 1 We first show that \mathfrak{M}^* is convex.

For this, consider $\alpha \in [0, 1]$ and $M, M' \in \mathfrak{M}^*$. Then, by definition of the normalization and by convexity of the exponential function,

$$\begin{aligned} e^{\gamma(\alpha M + (1-\alpha)M')} &= \int_{\mathcal{D}} e^{-\langle \alpha M + (1-\alpha)M', T(\mathbf{x}) \rangle_{\text{tr}} + \xi(\mathbf{x})} d\nu \\ &\leq \int_{\mathcal{D}} (\alpha e^{-\langle M, T(\mathbf{x}) \rangle_{\text{tr}} + \xi(\mathbf{x})} + (1-\alpha) e^{-\langle M', T(\mathbf{x}) \rangle_{\text{tr}} + \xi(\mathbf{x})}) d\nu \\ &= \alpha e^{\gamma(M)} + (1-\alpha) e^{\gamma(M')} < \infty. \end{aligned}$$

Hence, $\gamma(\alpha M + (1-\alpha)M') < \infty$, and thus, $\alpha M + (1-\alpha)M' \in \mathfrak{M}^*$. This concludes the proof of the first property.

Property 2 We now show that for any $M \in \mathfrak{M}^*$, the coordinates of $T(X)$ have moments of all orders with respect to f_M .

To this end, fix an $M \in \mathfrak{M}^*$. Since \mathfrak{M}^* is open, there is a neighborhood \mathfrak{M}_M of $0_{q \times q}$ such that $\{M - A : A \in \mathfrak{M}_M\} \subset \mathfrak{M}^*$. For any $A \in \mathfrak{M}_M$, the moment generating function of $T(X)$ is finite:

$$\mathbb{E}_M e^{\langle A, T(X) \rangle_{\text{tr}}} = \int_{\mathcal{D}} e^{-\langle M - A, T(\mathbf{x}) \rangle_{\text{tr}} + \xi(\mathbf{x}) - \gamma(M)} d\nu = e^{\gamma(M - A) - \gamma(M)} < \infty.$$

This is a sufficient condition for the existence of all moments of $T(X)$ (Shao 2003, Page 33) and thus concludes the proof of the second property. \square

A.2 Proof of Lemma 3.2

Proof of Lemma 3.2. The claim follows readily from Lemma 3.3, which is proved in the next section. Indeed, using the second derivatives stated in Lemma 3.3, we find for any

$M \in \mathfrak{M}^*$ and $M' \in \mathbb{R}^{q \times q}$,

$$\begin{aligned} & \sum_{i,j,k,l=1}^q M'_{ij} \frac{\partial}{\partial M_{ij}} \frac{\partial}{\partial M_{kl}} (\langle M, \bar{T}(\underline{\mathbf{x}}) \rangle_{\text{tr}} + \gamma(M)) M'_{kl} \\ &= n \sum_{i,j,k,l=1}^q M'_{ij} \mathbb{E}_M [(\bar{T}_{ij}(\underline{X}) - \mathbb{E}_M \bar{T}_{ij}(\underline{X}))(\bar{T}_{kl}(\underline{X}) - \mathbb{E}_M \bar{T}_{kl}(\underline{X}))] M'_{kl} \\ &= n \mathbb{E}_M \langle M', \bar{T}(\underline{X}) - \mathbb{E}_M \bar{T}(\underline{X}) \rangle_{\text{tr}}^2. \end{aligned}$$

The display implies that for any $M \in \mathfrak{M}^*$ and $M' \in \mathbb{R}^{q \times q}$,

$$\sum_{i,j,k,l=1}^q M'_{ij} \frac{\partial}{\partial M_{ij}} \frac{\partial}{\partial M_{kl}} (\langle M, \bar{T}(\underline{\mathbf{x}}) \rangle_{\text{tr}} + \gamma(M)) M'_{kl} \geq 0.$$

This ensures convexity, and thus concludes the proof of Lemma 3.2. \square

A.3 Proof of Lemma 3.3

Proof of Lemma 3.3. We prove the two claims in order.

Part 1 We start by taking the first derivative, showing that

$$\nabla_{ij} (\langle M, \bar{T}(\underline{\mathbf{x}}) \rangle_{\text{tr}} + \gamma(M)) = \bar{T}_{ij}(\underline{\mathbf{x}}) - \mathbb{E}_M \bar{T}_{ij}(\underline{X}),$$

where we use the shorthand notation $\nabla_{ij} := \frac{\partial}{\partial M_{ij}}$.

Since the trace is linear, the derivative of the first term is

$$\nabla_{ij} \langle M, \bar{T}(\underline{\mathbf{x}}) \rangle_{\text{tr}} = \bar{T}_{ij}(\underline{\mathbf{x}}).$$

For the second term, recall that the normalization γ is given by

$$\gamma(M) = \log \int_{\mathcal{D}} e^{-\langle M, T(\mathbf{x}) \rangle_{\text{tr}} + \xi(\mathbf{x})} d\nu.$$

Taking exponentials on both sides, we find

$$e^{\gamma(M)} = \int_{\mathcal{D}} e^{-\langle M, T(\mathbf{x}) \rangle_{\text{tr}} + \xi(\mathbf{x})} d\nu.$$

We can now take derivatives and get

$$\begin{aligned} e^{\gamma(M)} \nabla_{ij} \gamma(M) &= \int_{\mathcal{D}} \nabla_{ij} e^{-\langle M, T(\mathbf{x}) \rangle_{\text{tr}} + \xi(\mathbf{x})} d\nu \\ &= - \int_{\mathcal{D}} T_{ij}(\mathbf{x}) e^{-\langle M, T(\mathbf{x}) \rangle_{\text{tr}} + \xi(\mathbf{x})} d\nu, \end{aligned}$$

where we again use the linearity of the trace. Bringing the exponential factor back into the integral and using the assumed independence of the observations then yields

$$\nabla_{ij}\gamma(\mathbf{M}) = - \int_{\mathcal{D}} T_{ij}(\mathbf{x}) e^{-\langle \mathbf{M}, T(\mathbf{x}) \rangle_{\text{tr}} + \xi(\mathbf{x}) - \gamma(\mathbf{M})} d\nu = -\mathbb{E}_{\mathbf{M}} T_{ij}(X) = -\mathbb{E}_{\mathbf{M}} \bar{T}_{ij}(\underline{X}).$$

This provides the derivative for the second term. Collecting the pieces concludes the proof of the first part.

Part 2 We now compute the second derivative, showing that

$$\begin{aligned} \nabla_{ij}\nabla_{kl} (\langle \mathbf{M}, \bar{T}(\underline{\mathbf{x}}) \rangle_{\text{tr}} + \gamma(\mathbf{M})) \\ = \mathbb{E}_{\mathbf{M}} [(\bar{T}_{ij}(\underline{X}) - \mathbb{E}_{\mathbf{M}} \bar{T}_{ij}(\underline{X})) (\bar{T}_{kl}(\underline{X}) - \mathbb{E}_{\mathbf{M}} \bar{T}_{kl}(\underline{X}))], \end{aligned}$$

where we again use the shorthand notation $\nabla_{ij} = \frac{\partial}{\partial M_{ij}}$.

To prove this claim, recall that by Part 1,

$$\nabla_{kl} (\langle \mathbf{M}, \bar{T}(\underline{\mathbf{x}}) \rangle_{\text{tr}} + \gamma(\mathbf{M})) = \bar{T}_{kl}(\underline{\mathbf{x}}) - \mathbb{E}_{\mathbf{M}} \bar{T}_{kl}(\underline{X}).$$

Since the first term is independent of \mathbf{M} , we can focus on the second term. Independence of the observations and the model (2) provide

$$\mathbb{E}_{\mathbf{M}} \bar{T}_{kl}(\underline{X}) = \mathbb{E}_{\mathbf{M}} T_{kl}(X) = \int_{\mathcal{D}} T_{kl}(\mathbf{x}) e^{-\langle \mathbf{M}, T(\mathbf{x}) \rangle_{\text{tr}} + \xi(\mathbf{x}) - \gamma(\mathbf{M})} d\nu.$$

Taking derivatives, we find similarly as in Part 1

$$\begin{aligned} & - \nabla_{ij} \mathbb{E}_{\mathbf{M}} \bar{T}_{kl}(\underline{X}) \\ &= - \int_{\mathcal{D}} T_{kl}(\mathbf{x}) \nabla_{ij} e^{-\langle \mathbf{M}, T(\mathbf{x}) \rangle_{\text{tr}} + \xi(\mathbf{x}) - \gamma(\mathbf{M})} d\nu \\ &= - \int_{\mathcal{D}} T_{kl}(\mathbf{x}) (-T_{ij}(\mathbf{x}) - \nabla_{ij}\gamma(\mathbf{M})) e^{-\langle \mathbf{M}, T(\mathbf{x}) \rangle_{\text{tr}} + \xi(\mathbf{x}) - \gamma(\mathbf{M})} d\nu \\ &= - \int_{\mathcal{D}} T_{kl}(\mathbf{x}) (-T_{ij}(\mathbf{x}) + \mathbb{E}_{\mathbf{M}} T_{ij}(X)) e^{-\langle \mathbf{M}, T(\mathbf{x}) \rangle_{\text{tr}} + \xi(\mathbf{x}) - \gamma(\mathbf{M})} d\nu \\ &= \int_{\mathcal{D}} (T_{ij}(\mathbf{x}) - \mathbb{E}_{\mathbf{M}} T_{ij}(X)) (T_{kl}(\mathbf{x}) - \mathbb{E}_{\mathbf{M}} T_{kl}(X)) e^{-\langle \mathbf{M}, T(\mathbf{x}) \rangle_{\text{tr}} + \xi(\mathbf{x}) - \gamma(\mathbf{M})} d\nu \\ &= \mathbb{E}_{\mathbf{M}} [(T_{ij}(X) - \mathbb{E}_{\mathbf{M}} T_{ij}(X)) (T_{kl}(X) - \mathbb{E}_{\mathbf{M}} T_{kl}(X))] \\ &= n \mathbb{E}_{\mathbf{M}} [(\bar{T}_{ij}(\underline{X}) - \mathbb{E}_{\mathbf{M}} \bar{T}_{ij}(\underline{X})) (\bar{T}_{kl}(\underline{X}) - \mathbb{E}_{\mathbf{M}} \bar{T}_{kl}(\underline{X}))]. \end{aligned}$$

Plugging this in above concludes the proof of Part 2. □

B Full Algorithm for the maximum likelihood estimator

In this appendix, we present the full algorithm, which utilizes a backtracking line search to adaptively select step sizes and incorporate the applicable domain constraint. By convention, $g(\tilde{M})$ is infinite for $\tilde{M} \notin \mathfrak{M}$. The inequality of backtracking line search implies that $\tilde{M}_{k-1} - \eta \nabla \tilde{g}(\tilde{M}_{k-1}) \in \mathfrak{M}$. In a practical implementation, we multiple η by β until $\tilde{M}_{k-1} - \eta \nabla \tilde{g}(\tilde{M}_{k-1}) \in \mathfrak{M}$.

Algorithm 2: Solving for the maximum likelihood estimator with a backtracking line search

```

//  $\eta$  : initial step size
//  $\alpha, \beta$ : backtracking parameters
Input :  $\bar{T}(\underline{X}), \eta > 0, \alpha \in (0, 0.5), \beta \in (0, 1)$ 
Output:  $\hat{M}$ 
// Solve for  $M_0$ 
1  $M_0 \leftarrow \mathbf{0}_{p \times p}$ ;
2 for  $i = 1, \dots, p$  do
3    $(M_0)_{ii} \leftarrow \operatorname{argmin}_{m \in \mathbb{R}} \left\{ m \bar{T}_{ii}(\underline{X}) + \log \int \exp(-m T_{ii}(\mathbf{x}) + \xi(x_i)) dx_i \right\}$ ;
   // Generate sample set  $Y$  from  $f_{M_0} = \prod_{i=1}^p f_{(M_0)_{ii}}(x_i)$ 
4 for  $i = 1, \dots, p$  do
5    $\left[ \right.$  Generate 10,000 random samples from  $f_{(M_0)_{ii}}(x_i)$  for the  $i$ -th coordinate;
   // Apply gradient descent with a backtracking line search to (8)
6  $k \leftarrow 0$ ;
7  $\tilde{M}_k \leftarrow M_0$ ;
8 repeat
9    $k \leftarrow k + 1$ ;
10   $\nabla \tilde{g}(\tilde{M}_{k-1}) \leftarrow \bar{T}(\underline{X}) - \frac{\sum_{Z \in Y} T(Z) e^{-\langle \tilde{M}_{k-1} - M_0, T(Z) \rangle_{\text{tr}}}}{\sum_{Z \in Y} e^{-\langle \tilde{M}_{k-1} - M_0, T(Z) \rangle_{\text{tr}}}}$ ;
   // Select the stepsize adaptively using a backtracking line search
11  repeat
12     $\eta \leftarrow \beta \eta$ ;
13    until  $\tilde{g}(\tilde{M}_{k-1} - \eta \nabla \tilde{g}(\tilde{M}_{k-1})) \leq \tilde{g}(\tilde{M}_{k-1}) - \alpha \eta \|\nabla \tilde{g}(\tilde{M}_{k-1})\|^2$ ;
14     $\tilde{M}_k \leftarrow \tilde{M}_{k-1} - \eta \nabla \tilde{g}(\tilde{M}_{k-1})$ ;
15 until  $|\tilde{g}(\tilde{M}_k) - \tilde{g}(\tilde{M}_{k-1})| < 10^{-4}$ ;
16  $\hat{M} \leftarrow \tilde{M}_k$ ;

```

C Data Generation

Here we describe how to generate samples from an exponential trace model in the form of

$$f_{\mathbf{M}}(\mathbf{x}) = e^{-\langle \mathbf{M}, T(\mathbf{x}) \rangle_{\text{tr}} + \xi(\mathbf{x}) - \gamma(\mathbf{M})}.$$

Generating data from a multivariate distribution directly is difficult for moderate node numbers. Instead, we consider a Gibbs sampler to sample from the conditional distribution at each iteration. Conditioning on all the other variables \mathbf{x}_{-j} , the density of x_j is

$$f_{\mathbf{M}}(x_j \mid \mathbf{x}_{-j}) \sim e^{-M_{jj}T_{jj} - 2\sum_{k \neq j} M_{jk}T_{jk} - \xi(x_j)}.$$

We generate the conditional distribution using a slice sampler Neal (2003) with R package `MfUSampler` Mahani & Sharabiani (2014).

Note the slice sampler was designed for continuous variables. For discrete coordinates, we uniformly spread the probability in the spike at an integer c into the interval between c and $c + 1$. This defines a continuous density

$$f_{\mathbf{M}}(y_j \mid \mathbf{x}_{-j}) \sim e^{-M_{jj}\lfloor y_j \rfloor - 2\sum_{k \neq j} M_{jk}T_{jk}(\lfloor y_j \rfloor, x_k) - \xi(\lfloor y_j \rfloor)},$$

where $\lfloor y_j \rfloor$ represents the largest integer less than y_j . We sample from the above continuous density and take $\lfloor y_j \rfloor$ as the realization of a discrete x_j .